



**HAL**  
open science

## Long focal length high repetition rate femtosecond laser glass welding

Marion Gstalter, Grégoire Chabrol, Armel Bahouka, Kokou Dodzi Dorkenoo,  
Jean Luc Rehspringer, Sylvain Lecler

► **To cite this version:**

Marion Gstalter, Grégoire Chabrol, Armel Bahouka, Kokou Dodzi Dorkenoo, Jean Luc Rehspringer, et al.. Long focal length high repetition rate femtosecond laser glass welding. *Applied optics*, 2019, 58 (32), 10.1364/AO.58.008858 . hal-03078894

**HAL Id: hal-03078894**

**<https://hal.science/hal-03078894>**

Submitted on 16 Dec 2020

**HAL** is a multi-disciplinary open access archive for the deposit and dissemination of scientific research documents, whether they are published or not. The documents may come from teaching and research institutions in France or abroad, or from public or private research centers.

L'archive ouverte pluridisciplinaire **HAL**, est destinée au dépôt et à la diffusion de documents scientifiques de niveau recherche, publiés ou non, émanant des établissements d'enseignement et de recherche français ou étrangers, des laboratoires publics ou privés.

# Long focal length high repetition rate femtosecond laser glass welding

MARION GSTALTER,<sup>1,2,3</sup> GRÉGOIRE CHABROL,<sup>1,4</sup> ARMEL BAHOUKA,<sup>2</sup>  
KOKOU-DODZI DORKENOO,<sup>3</sup> JEAN-LUC REHSPRINGER,<sup>3</sup> AND SYLVAIN  
LECLER<sup>1\*</sup>

<sup>1</sup>*ICube, University of Strasbourg, UMR CNRS, Strasbourg, France*

<sup>2</sup>*IREPA LASER, Institut Carnot Mica., Boulevard Sébastien Brant, Illkirch, France*

<sup>3</sup>*Institut de Physique et Chimie des Matériaux de Strasbourg (IPCMS), UMR 7504 CNRS-Unistra, Strasbourg, France*

<sup>4</sup>*ECAM Strasbourg-Europe, Rue de Madrid, Schiltigheim, France*

\*[sylvain.lecler@icube.unistra.fr](mailto:sylvain.lecler@icube.unistra.fr)

**Abstract:** A long focal length focusing device is proposed for the process of glass welding by femtosecond laser pulses at high repetition rate and report on the significant advantages. The study is performed using a 100 mm focusing length F-theta lens. The results are compared to those obtained with high numerical aperture microscope objective. The long focal length with the associated Rayleigh length method allows a robust high process speed: welding at 1000 mm/s has been achieved, several order of magnitude larger compared to what was reported till now. Moreover, the heat accumulation process on a larger laser spot leads to a lower temperature increase after each pulse and thus a lower thermic gradient. As a result, the residual stress in the welding seams is reduced, preventing the formation of fractures inside the seams: mechanical resistance at 30 MPa has been measured

© 2019 Optical Society of America under the terms of the [OSA Open Access Publishing Agreement](#)

## 1. Introduction

Glass welding by femtosecond laser pulses is a recent method which has been developed to overcome the weaknesses of the conventional glass bonding technics [1, 2]. Classical processes such as adhesive bonding or fusing require either the addition of an adhesive material or high temperature. The first one limits the chemical and thermal resistance of the bonding and the second one is unsuitable for temperature sensitive material [3]. By comparison, glass welding by ultrashort laser pulses presents many advantages in term of mechanical, thermal and chemical resistance, control and precision, biocompatibility and process speed [4-6]. This method is particularly suitable for micro-welding applications, such as micro-optics, microfluidics or MEMS packaging [7].

Femtosecond laser glass welding relies on the irradiation of a volume at the interface of two glass plates in close contact with a focused laser beam, as illustrated in Fig. 1. Due to the low linear absorption at 1030 nm in our case, the beam can propagate through the first glass plate until high optical intensity is reached in the focused spot, generating nonlinear absorption of the laser energy [7]. The use of a high repetition rate laser (above 300 kHz for borosilicate glass) introduces thermal accumulation effects leading to a localized temperature increase of the glass in the focusing point up to its melting point [1]. The bonding is obtained during the fast cooling of the melting pool.

Probably due to the former difficulty in reaching the non-linear absorption threshold with "classic" lasers (pulse duration  $\geq$  ps), femtosecond laser glass bonding at high repetition rate has mainly been demonstrated using microscope objective with high numerical aperture (Fig. 2) [8]. The work presented in this paper demonstrates the benefits of using a scanner head containing a long focusing length lens with low numerical aperture (Fig. 3). At first glance, the welding process can be described similarly in both configurations: nonlinear absorption of the laser beam and thermal accumulation effect due to high repetition rate. The

volumetric fluency involved in the process is however much higher (around 100 times) in the case of a microscope objective than that of a scanner head.

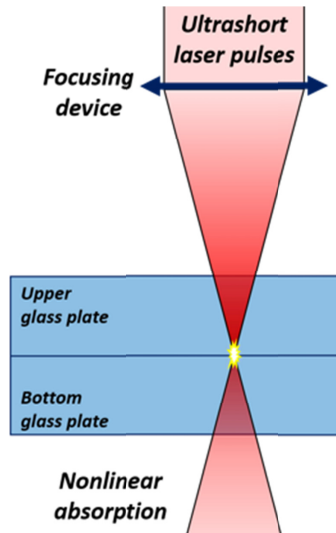


Fig. 1. Schematic view of our glass welding setup by femtosecond laser pulses.

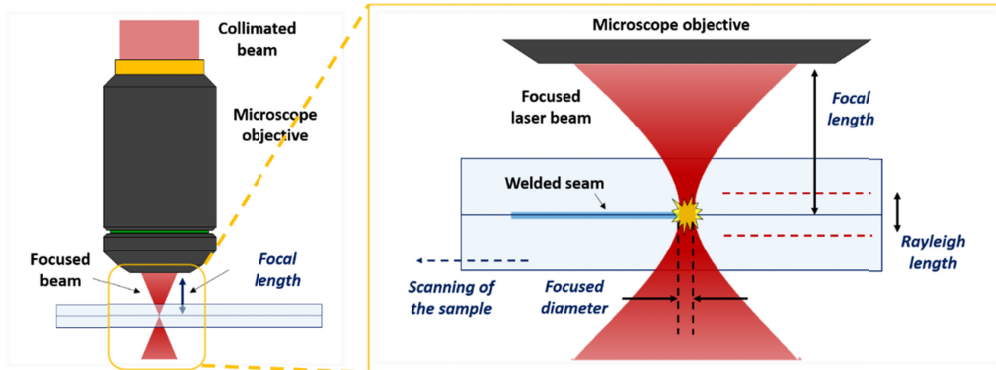


Fig. 2. Schematic view of the common glass welding process by femtosecond laser pulses using microscope objective.

This paper reports on the advantages of using a long focal length focusing device instead of using a microscope objective with high numerical aperture, in terms of industrial performance (welding speed) and welding quality (low residual stress). The discrepancy regarding the temperature dynamics will be presented so as to explain the different performances of the two techniques.

## 2. Experimental system

Please see the checklist in Section 3 that summarizes all of the style specifications.

### 2.1 Material

Experiments have been conducted on 700  $\mu\text{m}$  thin borosilicate glass plates (Mempax, Schott). The glass plates have a high surface quality with an arithmetic average roughness of 0.5 nm and a flatness of 2  $\mu\text{m}$ . This surface quality is suitable for obtaining local optical contact without the use of an external pressuring device [9]. However, air gaps of typically around 3  $\mu\text{m}$  between the two glass plates can be locally observed by the presence of interference fringes.

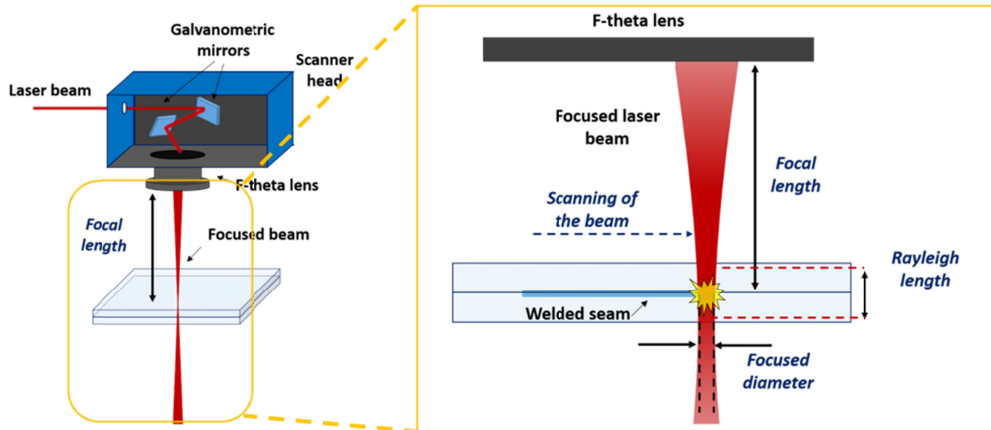


Fig. 3. Schematic view of glass welding by ultra-short laser pulses using a galvanometric head.

## 2.2 Laser system

The experiments have been carried out using an industrial laser station at IREPA LASER, developed specifically for micro-processing studies. This station is composed of an industrial high repetition rate laser from Amplitude System, tunable from 200 kHz up to 2 MHz, generating 300 fs duration pulses at a central wavelength of 1030 nm. The laser power can be adapted using an attenuator, composed by a half-waveplate and a prism polarizer, up to 25 W. The focusing device contains a 100 mm focusing length F-theta lens and galvanometric mirrors, and can be preceded by a beam expander to adjust the focused spot dimension. The diameter of the focused beam can be measured with a scanning split profiler with a precision of 2  $\mu\text{m}$  and can be adjusted between 30  $\mu\text{m}$  and 100  $\mu\text{m}$ .

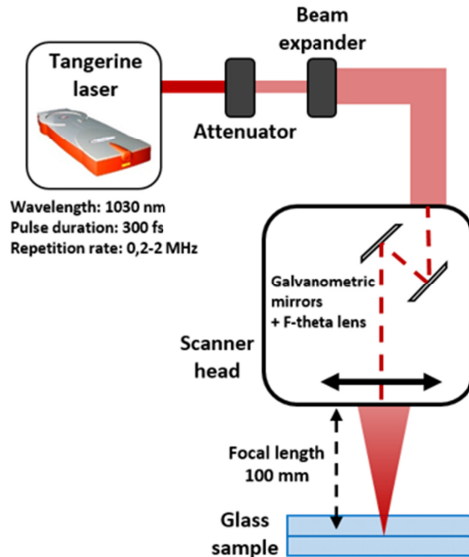


Fig. 4. Experimental setup for femtosecond laser glass welding with a long focal length focusing lens, as used in this paper.

Welding samples have been obtained by raster scanning in one pass a 30  $\mu\text{m}$  diameter focused beam along the interface, resulting in a number of pulses by spot of  $\Phi_0 f / v$  with  $\Phi_0$  the focused diameter,  $f$  the repetition rate and  $v$  the scanning speed of the laser beam. As an example, 300 pulses are delivered in one spot when welding with a 30  $\mu\text{m}$  diameter, at a

repetition rate of 500 kHz and at a scanning speed of 50 mm/s. Different parameters can be adjusted to evaluate their influence on the performance of the process. At a repetition rate of 2 MHz, the laser scanning speed can be set up to 1000 mm/s for an energy of 6  $\mu\text{J}$ . The large focal length makes this scanning speed possible, mainly due to the focus position robustness resulting from the long Rayleigh length (800  $\mu\text{m}$ ) of the beam, inducing a long material modification region (700  $\mu\text{m}$  measured). Such welding speed has never been reached using a microscope objective.

### 2.3 Characterization method

The welding process generates residual stresses inside the material, giving rise to structural modifications such as refractive index change or local birefringence. These residual stresses can be observed by photoelasticimetry, using an optical microscope with polarized light [10]. The microscope is composed of two polarizers set in crossed configuration, respectively called polarizer (P) and analyzer (A), between which the sample is inserted. The light transmitted through the system is observed as a function of the sample orientation (Fig. 5).

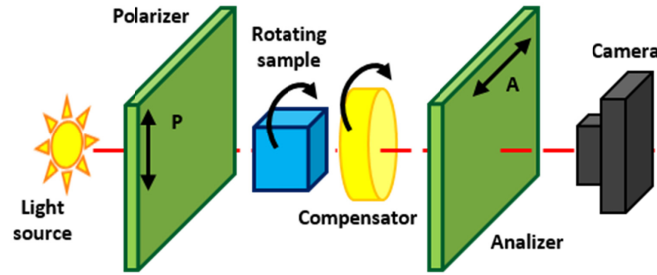


Fig. 5. Experimental setup for stress observation using photoelasticimetry.

A classical measurement method is implemented to determine the amount of laser-induced stress. A compensator plate (Leitz, Brace-Kohler compensator) is inserted between the sample and the analyzer. The rotation of the compensator plate introduces a tunable level of retardation. This known retardation allows to determine the level of birefringence introduced by the laser welding process as well as that of residual stress. The mechanical resistance of the welded samples has been measured by a tensile test.

### 3. Numerical model

A numerical model has been developed to estimate roughly the temperature increase induced by the thermal accumulation effect in the glass due to the absorption of the laser pulses. As described in detail below, this model is based on the underlying principles presented in other research papers on glass welding by ultrashort laser pulses [11, 12]. This simulation is of considerable interest to understand the physical mechanisms responsible for the glass welding process. It is not aimed to fully describe the welding process, but rather to identify the main tendencies.

Different studies describe absorption physical mechanisms and heat transport mechanisms. As the time constant for the absorption of the laser pulses of around a few picosecond is smaller than the one for thermal diffusion of a few microseconds, the temperature evolution process can be simulated by a simple thermal diffusion model with the laser pulse modelled as a heat source [11, 12]. As the pulse-to-pulse overlap is higher than 95 % in our case, to benefit from thermal accumulation, the translation of the beam can be neglected. A simplified model has been developed for a first approximation, considering stationary successive pulses irradiating the sample.

The heat transfer equation describes the temperature distribution  $T$  in space and time.

$$\rho C_p \frac{\partial T(r,z,t)}{\partial t} - \nabla(k \nabla T(r,z,t)) = Q(r,z,t) \quad (1)$$

This equation involves the thermal conductivity  $k$ , the material density  $\rho$ , and the specific heat capacity at constant pressure  $C_p$ . These parameters depend on temperature, but have been set as constant at first approximation without phase change. For borosilicate glass plates, the thermal conductivity is  $k = 1.12 \text{ W/(m.K)}$ , the density is  $\rho = 2200 \text{ kg/m}^3$  and the specific heat capacity is  $C_p = 820 \text{ J/(kg.K)}$ .

The heat source  $Q(r, z, t)$  describes the absorbed part of the energy in the material, and has been modelled as a 3D spatial and temporal Gaussian heat source.

$$Q(r, z, t) = Q_0 \exp\left(\frac{-2r^2}{r_s^2}\right) \exp\left(\frac{-2z^2}{Z_s^2}\right) \exp\left(\frac{-2t^2}{t_0^2}\right) \quad (2)$$

With

$$Q_0 = \frac{8E_0}{\pi^2 r_s^2 Z_s t_0} \quad (3)$$

The different parameters of the equation have been chosen according to the welding seams dimensions.  $Z_s = 200 \mu\text{m}$ , corresponds to the material modification length induced by our focused beam. Due to the non-linear absorption, the seam width observed,  $r_s = 4 \mu\text{m}$ , is different than the laser spot size.  $t_0$ , the pulse duration, has been set to 300 fs.

The simulation of this model reveals a low temperature increase of around  $200 \text{ }^\circ\text{C}$  after each pulse (Fig. 6-a), and confirms the influence of the thermal accumulation effect in the welding process. As the duration between two successive pulses ( $2 \mu\text{s}$ ) is smaller than the thermal diffusion inside the material (around  $100 \mu\text{s}$ ) [12], the temperature locally increases at each pulse arrival (around  $100 \text{ }^\circ\text{C}$  between two successive pulses at the beginning), up to the melting temperature of the glass (Fig. 7). This temperature evolution is low compared to the one given for a microscope objective (Fig. 6-b, with focal length  $f = 10 \text{ mm}$ ), where the induced temperature generated by one single pulse is directly well above the melting point of the glass (Fig. 7-b).

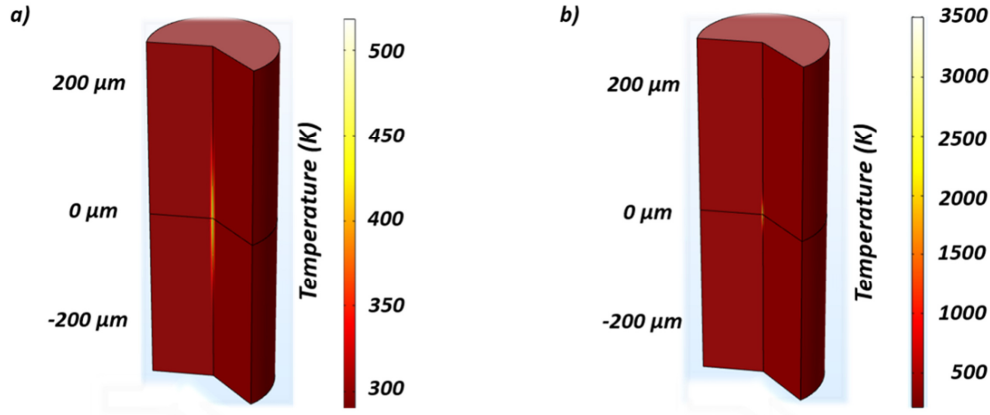


Fig. 6. Temperature distribution inside glass induced by the absorption of the first laser pulse, before thermal diffusion (1030 nm, 3  $\mu\text{J}$ , 300 fs), a) Heat source:  $Z_s = 200 \mu\text{m}$ ,  $r_s = 4 \mu\text{m}$ , generated by a scanner head, focal length  $f = 100 \text{ mm}$  and b) Heat source:  $Z_s = 50 \mu\text{m}$ ,  $r_s = 2 \mu\text{m}$ , generated by an optical microscope, focal length  $f = 10 \text{ mm}$ .

In other studies on the heat accumulation effect in the case of microscope objective, temperature increases from  $1600^\circ\text{C}$  (Fig. 6-b) to  $12000 \text{ }^\circ\text{C}$  have been simulated [11, 12]. For welding seams obtained using the F-theta lens, smaller temperature increases of around  $200 \text{ }^\circ\text{C}$  after one pulse have been observed from the simulations. This huge difference can be explained by the variation of the focused spot volume from a diameter of  $2 \mu\text{m}$  and a Rayleigh length below  $10 \mu\text{m}$  for a microscope objective to a diameter of  $30 \mu\text{m}$  and a Rayleigh length of  $800 \mu\text{m}$  with the F-theta lens. This demonstrates a different mechanism of heat accumulation effect: in the case of microscope objective, the accumulation effect is used

to spatially increase the melted area, whereas for the F-theta lens, the thermal accumulation effect is used to increase the temperature of the entire volume.

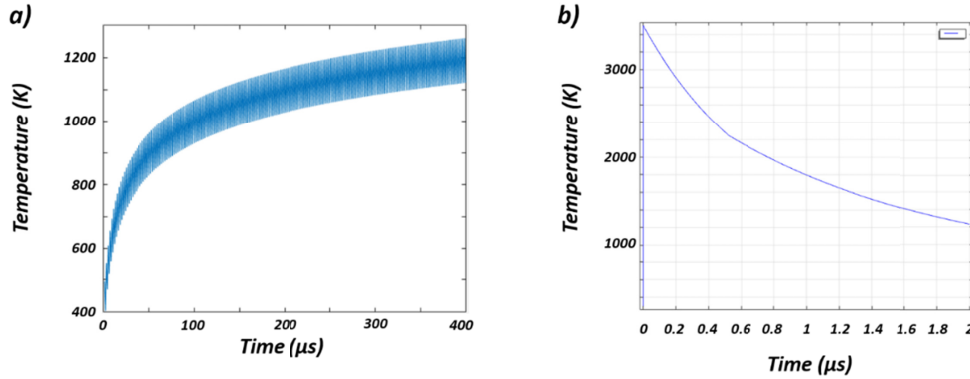


Fig. 7. Temporal temperature evolution for 3  $\mu\text{J}$ , 300 fs, 500 kHz pulses, showing: a) the slow thermal accumulation effect inside the material in the configuration with the F-theta lens, focal length  $f=100$  mm (Heat source:  $Z_s = 200 \mu\text{m}$ ,  $r_s = 4 \mu\text{m}$ ), b) the fast temperature increase with a microscope objective, focal length  $f=10$  mm (Heat source:  $Z_s = 50 \mu\text{m}$ ,  $r_s = 2 \mu\text{m}$ ).

## 4. Results and discussion

### 4.1 High welding speed

As can be seen in the following paragraphs, the use of a long focal length focusing device brings one main advantage in term of industrial process: the possibility to reach a very high scanning speed, also possible due to an easy positioning of the laser beam at the glass plates interface. Namely, an interest of the 100 mm F-theta lens is the long Rayleigh length available, almost 800  $\mu\text{m}$  in our case. Long Rayleigh length generates elongated welding seams compared to those obtained by a microscope objective. With suitable scanning speed and energy, at a repetition rate of 2 MHz, welding seams deeper than 200  $\mu\text{m}$  have been measured. This elongated welded area allows a large freedom of positioning around the interface. Welding can even be obtained with more than  $\pm 100 \mu\text{m}$  uncertainties in positioning, as described in the Table 1, making the process very robust.

Table 1. Tolerance in positioning for different laser mean power at a scanning speed of 50 mm/s

Power (W)	3.1	4.4	6.0	12.0
Tolerance ( $\mu\text{m}$ )	$\pm 75$	$\pm 75$	$\pm 100$	$\pm 200$

In most of the current glass welding demonstration using femtosecond laser pulses focused by a microscope objective, the scanning speed is limited to around 1-10 mm/s [1], which is already much higher than the first demonstration with low repetition rate laser [7]. In our configuration, with a high repetition rate laser system and a long focal length focusing device, it is possible to reach a scanning speed of up to 200 mm/s with low energy, i.e. around 3  $\mu\text{J}$ . Increasing the repetition rate to 2 MHz and the pulse energy to 10  $\mu\text{J}$ , successful welding has been obtained for scanning speeds of up to 1000 mm/s.

### 4.2 Low residual stress

The model developed to estimate the evolution of the temperature distribution ~~evolution~~ has been presented in Section 3. Compared to the temperature distribution simulated for glass

welding with microscope objective, the speed of the temperature increases and the gradients induced by a long focal length focusing device are clearly much smaller.

The residual stresses induced by the welding process [10] are thus expected to be smaller in the case of the scanner head. The local birefringence in the glass introduced by the residual stresses are observed by photoelasticimetry, as described in Section 2.3. The orientation of the residual stresses can be determined by the rotation of the sample, as can be seen in Fig. 8, where the same area is observed, rotated at 45°. When the welded seams are parallel or orthogonal to the crossed polarizer-analyzer system, the field appears dark: the stresses are parallel or orthogonal to the incident polarization. On the opposite, the contrast is maximum when the seams direction is rotated by 45°: the stresses are at 45° to the incident polarization.

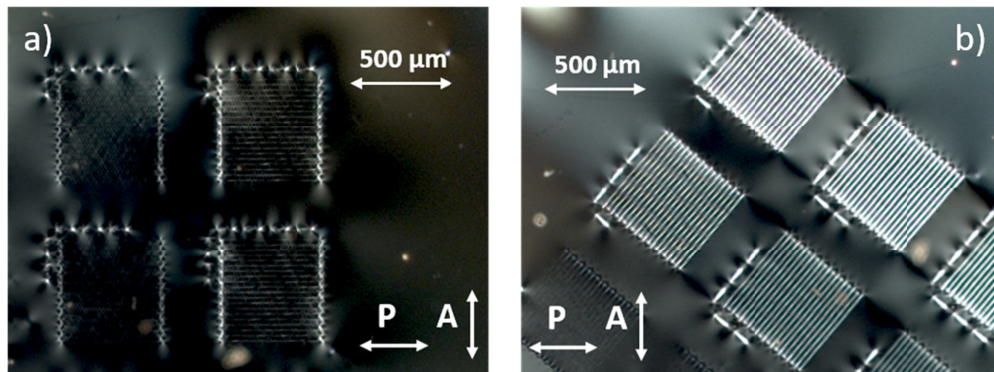


Fig. 8. Observation by photoelasticimetry of welding seams: determination of the residual stress orientation by the rotation of the sample. (500 kHz, 100 mm/s, 3-6  $\mu$ J)

The addition of a first-order waveplate, according to the standard test method for photoelastic determination of residual stress (C 978-04 standard), shows that welding seams undergo stretching stress orthogonal to the scanning direction [10]. The residual stress has been measured lower than 60 MPa for low energy close to the absorption threshold [10]. Just for comparison, this is well below the internal residual stress amount of 1 GPa inducing breakage [13].

#### 4.3 High quality welding seams

The presence of cracks along or at the edges of the welding seams performed using microscope objective can be induced by either an excess or an overlap of the residual stress inside the welding seams [1]. On the other hand, the low residual stress process, made possible by the use of a long focal length focusing device, allows for lower risks of fractures and defaults in the welding seams. By adapting the pulse energy, it is possible to obtain homogeneous and crack-free welding seams. The side view of welding seams obtained by the scanner head (Fig. 9) shows a homogeneous section without visible defaults.

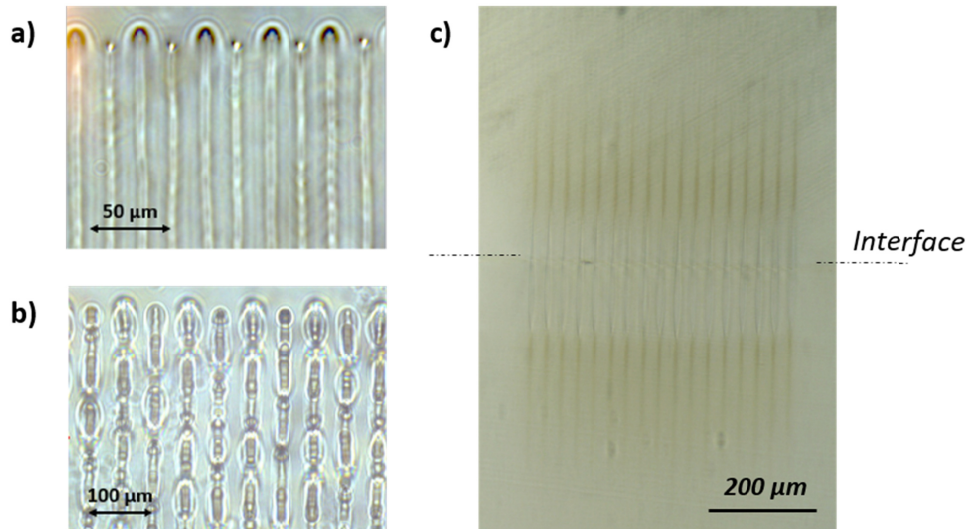


Fig. 9. Top and side views of welding seams: a) top view of homogeneous welding seams (500 kHz, 100 mm/s, 5  $\mu$ J), b) top view of inhomogeneous welding seams (2 MHz, 100 mm/s, 2.8  $\mu$ J), c) side view of homogeneous welding seams (500 kHz, 50 mm/s, 4.8  $\mu$ J).

The mechanical resistance of the welded samples has been measured for different laser parameters. Breakout force up to 200 N has been measured, resulting in a mechanical strength of 30 MPa. These values are of the same order of magnitude than the best mechanical strength of welded samples realized with microscope objectives without burst mode [14, 15]. They may still be improved using burst mode or optimized patterns [16]. Depending on the laser parameters, different morphologies of the welding seams after breakout can be observed. Either the seams can be ripped off, or the material around the seams can be removed from one plate and stay welded to the other plate, as shown in Fig. 10. The thermal resistance has been investigated by inducing successfully thermal shocks on the welded samples. For this, the samples have been deposited in an oven at ambient temperature and heated up to the test temperature, before being immersed in water at ambient temperature. Thermal shock up to 300°C have thus been successfully implemented on welded samples.

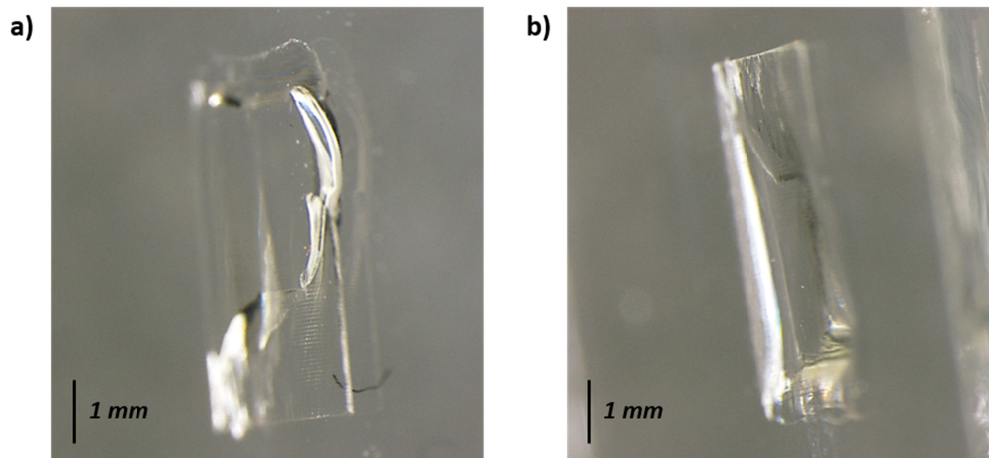


Fig. 10. Macroscopic view of a welding area after the tensile test: a) first glass plates showing a bulging of the glass material above the welding seams, b) second glass plates showing the corresponding hole in the welding area.

## 5. Conclusion

Femtosecond laser glass welding has been demonstrated using a long focal length lens integrated in a scanner head instead of the more conventional microscope objectives with high numerical aperture. The welding principle can be described similarly for both methods, relying on melting due to thermal accumulation effect. However, the temperature dynamics are completely different. In the case of a long focal length lens, the large focusing diameter generated a lower temperature increase by pulse. This smooth temperature dynamics reduces the residual stress induced in the welding seams and limits the risk of fracture in the glass material. The use of a long focal length lens also offers further advantages for an industrial process. The long working distance, corresponding to long Rayleigh length, reduces the difficulties involved in positioning the focusing spot on the interface. Thus, a large attainable welding scanning speed of up to 1000 mm/s has been obtained, thus being a great advantage in terms of industrialization. The mechanical and thermal resistance of the samples are besides reasonable for a welding process, with a tensile strength of 30 MPa and the ability to sustain thermal shocks of 300 °C.

## Funding

This work has been supported by French ANRT.

## References

1. S. Richter, F. Zimmermann, A. Tünnermann and S. Nolte, "Laser welding of glasses at high repetition rates – Fundamentals and prospects," *Optics & Laser Technology* **83**, 59-66 (2016).
2. Y. Okamoto, I. Miyamoto, K. Cvecek, A. Okada, K. Takahashi, M. Schmidt, "Evaluation of molten zone in micro-welding of glass by picosecond pulsed laser", *Journal of Laser Micro/Nanoengineering*. **8** (1), 65-69 (2013).
3. D. Hülsenberg, A. Harnisch, A. Bismarck, in *Microstructuring of glasses*, ed. By D. Hülsenberg, A. Harnisch (Springer Ser. Mater.Science, 2008), p. 263
4. F. Zimmermann, S. Richter, S. Döring, A. Tünnermann, S. Nolte, "Ultrastable bonding of glass with femtosecond laser bursts", *Applied Optics* **52** (6), 1149-1154 (2013).
5. R. Carter, J. Chen, J.D. Shephard, R.R. Thomson, D.P. Hand, "Picosecond laser micro-welded similar and dissimilar material", Paper presented at 15<sup>th</sup> International Symposium on Laser Precision Microfabrication, Vilnius, Lithuania (2014).
6. K. Cvecek, R. Odato, S. Dehmel, I. Miyamoto, M. Schmidt, "Gap bridging in joining of glass using ultra short laser pulses", *Optics express* **23** (5), 5681-5693 (2015).
7. T. Tamaki, W. Watanabe, J. Nishii, K. Itoh, "Welding of transparent materials using femtosecond laser pulses", *Japanese Journal of Applied Physics* **44** (20), 687-689 (2005).
8. G. Zhang, R. Stoian, W. Zhao, G. Cheng, "Femtosecond laser Bessel beam welding of transparent to non-transparent materials with large focal-position tolerant zone" *Optics Express* vol. 26, n° 2, p. 917-926 (2018).
9. K. Cvecek, I. Miyamoto, J. Strauss, M. Wolf, T. Frick, M. Schmidt, "Sample preparation method for glass welding by ultrashort laser pulses yields higher seam strength" *Applied Optics* **50**, 1941 (2011).
10. M. Gstalter, G. Chabrol, A. Bahouka, L. Serreau, J-L. Heitz, G. Taupier, K-D. Dorkenoo, J-L. Rehspringer, S. Lecler, "Stress induced birefringence control in femtosecond laser glass welding" *Applied Physics A* **123** (714), (2017).
11. I. Miyamoto, A. Horn, J. Gottmann, D. Wortmann, F. Yoshino, "Fusion welding of glass using femtosecond laser pulses with high-repetition rates" *J. of Laser Micro/Nanoeng.* **2** (1), 57-63 (2007).
12. S. Richter, Ph.D. thesis, "Direct laser bonding of transparent materials using ultrashort laser pulses at high repetition rates", University of Friedrich-Schiller, Jena, (2014).
13. T.J. Holmquist, A. A. Wereszczak, "The internal tensile strength of a borosilicate glass determined from laser shock experiments and computational analysis", *International Journal of Applied Glass Science* **5** (4), 345-352 (2014).
14. D. Hélie, S. Gouin, R. Vallée, "Assembling an endcap to optical fibers by femtosecond laser welding and milling", *Optical Materials Express* **3** (10), 1742-1754 (2013).
15. K. Sugioka, M. Iida, H. Takai, K. Midorikawa, "Efficient microwelding of glass substrates by ultrafast laser irradiation using a double-pulse train", *Optics Letters* **36** (14), 2734-2736 (2011).
16. S. Richter, S. Nolte, A. Tünnermann, "Ultrashort pulse laser welding - a new approach for high-stability bonding of different glasses", *Physics Procedia* **39**, 556-562 (2012).